Frequency resolved transverse mode instability in rod fiber amplifiers

Johansen, Mette Marie; Laurila, Marko; Maack, Martin D.; Noordegraaf, Danny; Jakobsen, Christian; Alkeskjold, Thomas Tanggaard; Lægsgaard, Jesper

Published in:
Optics Express

Link to article, DOI:
10.1364/OE.21.021847

Publication date:
2013

Document Version
Publisher's PDF, also known as Version of record

Frequency resolved transverse mode instability in rod fiber amplifiers

Mette Marie Johansen,[1*] Marko Laurila,[2] Martin D. Maack,[2] Danny Noordegraaf,[2] Christian Jakobsen,[2] Thomas Tanggaard Alkeskjold,[2] and Jesper Lægsgaard[1]

[1]*DTU Fotonik, Technical University of Denmark, Ørsteds Plads building 343, 2800 Kgs. Lyngby, DK-Denmark*
[2]*NKT Photonics A/S, Blokken 84, 3460 Birkerød, DK-Denmark*
[*]*mmajo@fotonik.dtu.dk*

Abstract: Frequency dynamics of transverse mode instabilities (TMIs) are investigated by testing three 285/100 rod fibers in a single-pass amplifier setup reaching up to ~200W of extracted output power without beam instabilities. The pump power is increased well above the TMI threshold to uncover output dynamics, and allowing a simple method for determining TMI threshold based on standard deviation. The TMI frequency component is seen to appear on top of system noise that may trigger the onset. A decay of TMI threshold with test number is identified, but the threshold is fully recovered between testing to the level of the pristine fiber by thermal annealing the fiber output end to 300°C for 2 h.

OCIS codes: (060.2280) Fiber design and fabrication; (060.2320) Fiber optics amplifiers and oscillators; (060.4005) Microstructured fibers; (140.6810) Thermal effects.

References and links

1. D. J. Richardson, J. Nilsson, and W. A. Clarkson, "High power fiber lasers: current status and future perspectives [Invited]," J. Opt. Soc. Am. B **27**(11), B63–B92 (2010).
2. T. T. Alkeskjold, M. Laurila, L. Scolari, and J. Broeng, "Single-mode ytterbium-doped large-mode-area photonic bandgap rod fiber amplifier," Opt. Express **19**(8), 7398–7409 (2011).
3. M. Laurila, M. M. Jørgensen, K. R. Hansen, T. T. Alkeskjold, J. Broeng, and J. Lægsgaard, "Distributed mode filtering rod fiber amplifier delivering 292W with improved mode stability," Opt. Express **20**(5), 5742–5753 (2012).
4. C.-H. Liu, G. Chang, N. Litchinitser, D. Guertin, N. Jacobsen, K. Tankala, and A. Galvanauskas, "Chirally Coupled Core Fibers at 1550-nm and 1064-nm for Effectively Single-Mode Core Size Scaling," in *Conference on Lasers and Electro-Optics/Quantum Electronics and Laser Science Conference and Photonic Applications Systems Technologies*, OSA Technical Digest Series (CD) (Optical Society of America, 2007), paper CTuBB3.
5. F. Jansen, F. Stutzki, H.-J. Otto, M. Baumgartl, C. Jauregui, J. Limpert, and A. Tünnermann, "The influence of index-depressions in core-pumped Yb-doped large pitch fibers," Opt. Express **18**(26), 26834–26842 (2010).
6. D. C. Brown and H. J. Hoffman, "Thermal, stress, and thermo-optic effects in high average power double-clad silica fiber lasers," IEEE J. Quantum Electron. **37**(2), 207–217 (2001).
7. M.-A. Lapointe, S. Chatigny, M. Piché, M. Cain-Skaff, and J.-N. Maran, "Thermal effects in high power cw fiber lasers," Proc. SPIE **7195**, 71951U, 71951U-11 (2009).
8. J. Limpert, T. Schreiber, A. Liem, S. Nolte, H. Zellmer, T. Peschel, V. Guyenot, and A. Tünnermann, "Thermo-optical properties of air-clad photonic crystal fiber lasers in high power operation," Opt. Express **11**(22), 2982–2990 (2003).
9. A. V. Smith and J. J. Smith, "Mode instability in high power fiber amplifiers," Opt. Express **19**(11), 10180–10192 (2011).
10. T. Eidam, C. Wirth, C. Jauregui, F. Stutzki, F. Jansen, H.-J. Otto, O. Schmidt, T. Schreiber, J. Limpert, and A. Tünnermann, "Experimental observations of the threshold-like onset of mode instabilities in high power fiber amplifiers," Opt. Express **19**(14), 13218–13224 (2011).
11. B. Ward, C. Robin, and I. Dajani, "Origin of thermal modal instabilities in large mode area fiber amplifiers," Opt. Express **20**(10), 11407–11422 (2012).
12. H.-J. Otto, F. Stutzki, F. Jansen, T. Eidam, C. Jauregui, J. Limpert, and A. Tünnermann, "Temporal dynamics of mode instabilities in high-power fiber lasers and amplifiers," Opt. Express **20**(14), 15710–15722 (2012).
13. F. Stutzki, H.-J. Otto, F. Jansen, C. Gaida, C. Jauregui, J. Limpert, and A. Tünnermann, "High-speed modal decomposition of mode instabilities in high-power fiber lasers," Opt. Lett. **36**(23), 4572–4574 (2011).
14. C. Jauregui, T. Eidam, J. Limpert, and A. Tünnermann, "The impact of modal interference on the beam quality of high-power fiber amplifiers," Opt. Express **19**(4), 3258–3271 (2011).
15. K. R. Hansen, T. T. Alkeskjold, J. Broeng, and J. Lægsgaard, "Thermally induced mode coupling in rare-earth doped fiber amplifiers," Opt. Lett. **37**(12), 2382–2384 (2012).

#191938 - $15.00 USD Received 7 Jun 2013; revised 27 Aug 2013; accepted 4 Sep 2013; published 10 Sep 2013

16. K. R. Hansen, T. T. Alkeskjold, J. Broeng, and J. Lægsgaard, "Theoretical analysis of mode instability in high-power fiber amplifiers," Opt. Express **21**(2), 1944–1971 (2013).
17. M. M. Johansen, K. R. Hansen, M. Laurila, T. T. Alkeskjold, and J. Lægsgaard, "Estimating modal instability threshold for photonic crystal rod fiber amplifiers," Opt. Express **21**(13), 15409–15417 (2013).
18. L. Dong, "Stimulated thermal Rayleigh scattering in optical fibers," Opt. Express **21**(3), 2642–2656 (2013).
19. NKT Photonics A/S, "Ytterbium Doped Double Clad Fibers With Large Mode Area," <http://nktphotonics.com/side5319.html> (2 January 2013). http://nktphotonics.com/side5319.html.
20. I. Manek-Hönninger, J. Boullet, T. Cardinal, F. Guillen, S. Ermeneux, M. Podgorski, R. Bello Doua, and F. Salin, "Photodarkening and photobleaching of an ytterbium-doped silica double-clad LMA fiber," Opt. Express **15**(4), 1606–1611 (2007).
21. M. Leich, U. Röpke, S. Jetschke, S. Unger, V. Reichel, and J. Kirchhof, "Non-isothermal bleaching of photodarkened Yb-doped fibers," Opt. Express **17**(15), 12588–12593 (2009).
22. M. Leich, S. Jetschke, S. Unger, and J. Kirchhof, "Temperature influence on the photodarkening kinetics in Yb-doped silica fibers," J. Opt. Soc. Am. B **28**(1), 65–68 (2011).

1. Introduction

Ytterbium-doped silica based fiber lasers and amplifiers currently undergo significant improvements concerning beam quality performance and extractable average and peak power [1]. High pulse energies and peak powers require large effective area and new fiber designs are being investigated [2–5]. As state of the art large mode area (LMA) fiber amplifier can extract 100s of Watts per unit length, thermal-optic effects causing a thermally induced refractive index increment significantly influences the waveguiding mechanisms [6–8]. The index perturbations can cause very LMA fibers to support higher order modes (HOMs) at high power operation which can lead to mode degradation, and eventually transverse mode instability (TMI) that sets in at a threshold power level [9–11]. The temporal characteristics of TMIs reveal rapid fluctuating beam output on the ms time scale, where the fundamental mode (FM) and the first HOM interact [12]. FM and HOM interactions significantly degrade the beam quality, where the initially Gaussian like mode profile starts to fluctuate as TMIs set in. TMIs are often the first nonlinear effect to set in for very LMA fibers in high power amplifier and laser systems, and appear when the extracted average output power reaches a certain threshold. Currently TMIs set the upper limit for power scaling, and understanding the origin and mechanisms behind are important for future mitigation strategies. TMI can be observed with a standard CCD camera, but typically the refresh rate is too low to resolve the temporal dynamics [12,13]. Thus quantifying the underlying output evolution is impossible, and measuring the exact TMI threshold becomes extremely challenging. A simple and cheap method to detect TMI formation and evolution is required to quantify origin and dynamics. Different numerical models have been used to understand and explain the origin of TMIs ranging from heavy beam propagation models [9,11,14] to simpler semi-analytic models [15–18]. However the models have dissimilarities indicating a need for thorough experimental investigations of TMI.

In this work, we experimentally investigate the onset of TMIs as well as the frequency dynamics in different regimes of TMIs. We use a batch of three rods of the commercially available DC-285/100-PM-Yb-ROD [19] (285/100) fiber, see Fig. 1, which we test in a single pass amplifier setup reaching extracted output power levels well above 200 W. This fiber has a very large core of approximately 100 μm diameter, and HOMs can be excited by a misaligned seed coupling. This makes these rods particularly interesting for considering TMIs that require guidance of the first HOM. We consider the frequency evolution of the output with increasing pump power, i.e. increasing extracted output power, to uncover underlying dynamics by imaging a fraction of the mode profile onto a photodiode. This can help to identify important fiber properties and system parameters for future mitigation strategies. We also investigate the possibility to measure the TMI threshold by considering the standard deviation to efficiently detect mode movement, similar to Otto et *al.* [12], which leads to a new definition of the TMI threshold. The recorded output spectra are converted into spectrograms showing the frequency evolution of the modal output as a function of increasing extracted output power. A total of 6 spectrograms are presented each containing a significant amount of data, which we believe is useful for revealing the cause of TMI. We consider three 285/100 rod fibers that each undergoes the same procedure outlined in Sec. 2 to be able to

#191938 - $15.00 USD Received 7 Jun 2013; revised 27 Aug 2013; accepted 4 Sep 2013; published 10 Sep 2013

indentify similarities and draw general conclusions. A large number of tests are performed on each fiber, as well as one annealing step to recover the fibers to their pristine state, after which the fibers again undergo a large number of tests.

Previous experiments have shown that the TMI threshold decreases during operation as the threshold is reached multiple times, and that the initial threshold can be recovered by blue light photobleaching [3]. The threshold degradation indicates a memory effect in the fiber, which can be due to increased absorption or a permanent inscription of refractive index perturbations related to photodarkening. Photodarkening related color centers can be removed/reduced by UV photobleaching or thermal annealing [20–22].

The degradation of threshold is investigated during testing of each fiber by increasing the extracted output power well above the TMI threshold level and repeating the same measurement 10 – 15 times, denoted a "TMI repeat", see Table 1. This testing is initially performed on three pristine 285/100 rod fibers in a high power amplifier setup. After TMI repeat 1, 50 cm of the fiber output end is baked in an oven (Carbolite Horizontal CTF 1200) at 300°C for 2 h, i.e. half the fiber, and left to cool inside the oven to relax internal stresses, which results in a slow cool down annealing process, denoted "TMI anneal". Again a TMI repeat is performed consisting of 10 – 15 tests, to test the new evolution of the modal output and determine the TMI threshold, outlined in Table 1. For each rod fiber 20 – 30 measurements of TMI is performed, that gives a total of 80 measurements of TMI characteristics for all three 285/100 rod fibers (FUT1, FUT2, and FUT3). Table 1 outlines the experimental procedure with different tests indexed according to the FUT, the procedure step and the repeat test number. For example, TMI repeat test 8 in the second TMI repeat of FUT2 is denoted "FUT2-C8".

Table 1. Experimental Procedure for Test Fibers FUT1, FUT2, and FUT3.

Designator	Experimental procedure
A	TMI repeat 1
	1 2 3 4 5 6 7 8 9 10 11 12 13 14 15
B	TMI anneal
C	TMI repeat 1
	1 2 3 4 5 6 7 8 9 10 11 12 13 14 15

2. Experimental setup

The 285/100 rod fiber is backward pumped with a 976nm pump and seeded by a 1032nm fiber based ps seed. The extracted output power is measured using a dichroic mirror to reflect the signal to a power meter and a beam splitter (BS) for beam diagnostics. The mode profiles are imaged by a CCD camera (Spiricon GRAS20). A part of the mode profile is detected by placing a pinhole in front of a photodiode (PD) and processed by an oscilloscope (PicoScope 3204A). A schematic illustration of the setup is seen in Fig. 1. This simple measurement setup enables an efficient method of attaining information about the modal composition of the output, and allows simple studies of TMIs. The DC component of the photodiode signal represents the average power and increases with increasing output power. The AC component is low pass filtered ($f < 1.9$ MHz) to remove frequency components from the laser repetition

#191938 - $15.00 USD Received 7 Jun 2013; revised 27 Aug 2013; accepted 4 Sep 2013; published 10 Sep 2013

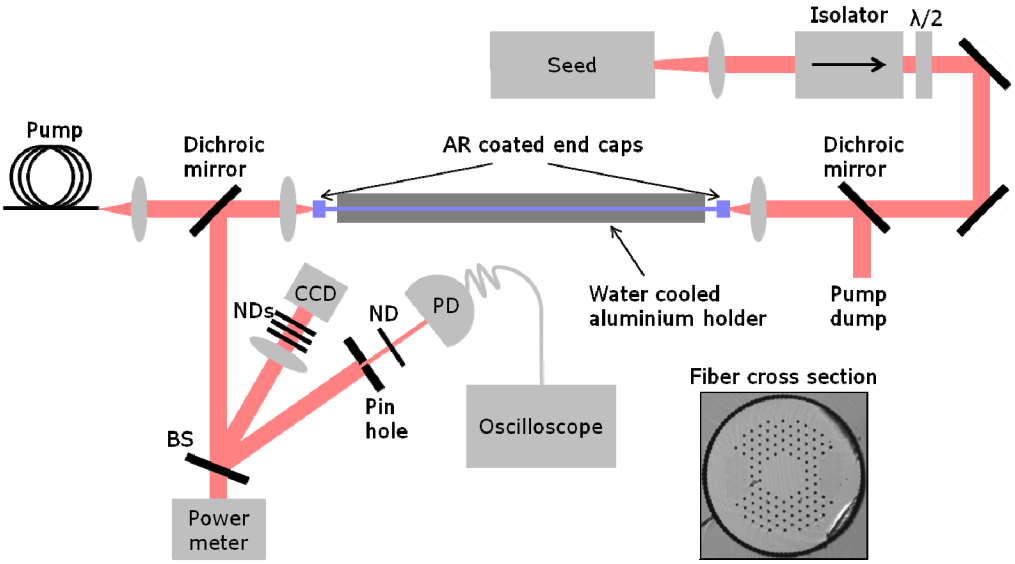

Fig. 1. Schematic illustration of the setup and the 285/100 rod fiber cross section in the lower right corner.

rate (40MHz) and remains small as long as the output mode is temporarily stable i.e. operates in the FM. The AC components start to increase when the mode fluctuations between the FM and HOM set in.

A time trace of the pinholed beam is recorded for every ~3 W of increased extracted output power of the 2nd, 8th, and 15th TMI test of each TMI repeat with FUT1 (i.e. FUT1-A2, FUT1-A8, FUT1-A15, FUT1-C2, FUT1-C8, FUT1-C15). The time trace is Fourier transformed to attain a frequency spectrum corresponding to a specific signal power. All the spectra from one TMI test (e.g. FUT1-A2) are plotted together as a spectrogram showing the output spectra normalized to the maximum signal power of that test in dB as a function of extracted output power and frequency. The spectrograms reveal the frequency evolution with increased output power, and are compared with the measured standard deviation of the pinholed beam to define the onset of TMIs.

3. Transverse mode instability onset and dynamics

The spectrograms recorded for FUT1 are considered in this section and reveal the frequency evolution of the recorded output of the pinholed photodiode with increased pump. Figure 2 shows the frequency spectrogram for extracted output power above 100 W of FUT1-A2. The standard deviation measured by the photodiode and oscilloscope is plotted on the same power scale on the right in Fig. 2. Up to 180 W of extracted output power, the DC component, which represents the FM signal, dominates the spectrum, and is visible in the spectrogram as the sharp line centered at 0 Hz. Above 180 W, TMI sets in having a clear frequency component of 360 Hz with also higher harmonics of that component at 720 Hz, 1080 Hz, and 1440 Hz. This is caused by beam fluctuations between the FM and first HOM, that are very obvious in the spectrogram and also visible by the CCD camera, but can be difficult to detect due to the camera's slow refresh rate. The TMI frequency components become power dependant above the TMI threshold of 180 W, where the peaks drift to higher frequencies with increased signal power. Otto et *al.* [12] have reported on temporal peak fluctuations, which could be related. We believe that the frequency drift is caused by continuous waveguide perturbations with increased output power due to the thermo-optic effect and possibly also temperature dependent material constants. At around 200 W, new frequency components enter the spectrogram also with visible higher harmonics, and more

#191938 - $15.00 USD Received 7 Jun 2013; revised 27 Aug 2013; accepted 4 Sep 2013; published 10 Sep 2013

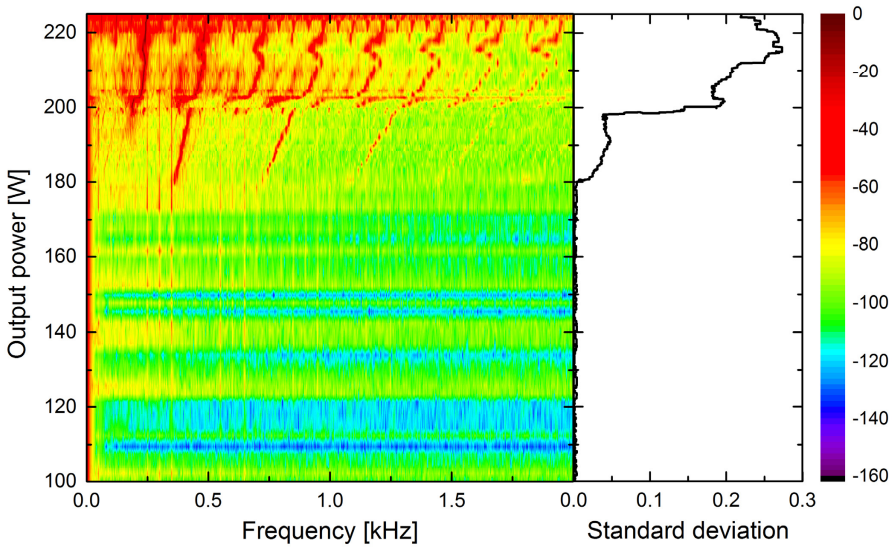

Fig. 2. Data for FUT1-A2. Fourier transformed normalized spectrogram plotted in dB for the extracted output power as a function of frequency. The standard deviation is plotted on equal power scale to the right.

lines enter again at 220 W, where after the TMI spectrogram becomes more continuous in nature as a white light span of frequencies.

Closely spaced vertical lines are observed in the spectrogram that seem independent of output power and stays constant in frequency. These lines are spaced with 50 Hz and are speculated to originate from the European grid frequency. At 180 W, where the TMIs set in with frequency components of 360 Hz, 720 Hz, 1080 Hz, and 1440 Hz, it seems as the main TMI frequency appear on top of a suspected vertical "electrical noise line". It is suspected that system dependent noise can work as a trigger for TMI, and thus the threshold level becomes noise dependent, which has also been demonstrated in numerical work [15,16].

The standard deviation in Fig. 2 is approximately zero below 180 W of extracted output power identified as a stable regime. At 180 W the standard deviation grows abrupt when TMIs set in reaching the so called transient regime with discrete frequency components followed by the more chaotic regime characteristic of a continuous frequency output, which will become more apparent in the following spectrograms for FUT1. The TMI threshold is clearly defined at 180 W of extracted output power from the abrupt increase in standard deviation when comparing to the clear appearance of an extra discrete frequency peak in the spectrogram.

The background level in the stable regime fluctuates between ~80 dB – 150 dB in Fig. 2 with recorded output power and is seen as horizontal lines of varying color. This is related to the photodiodes measurement uncertainty, since these values are estimated to be below the dynamic range, and therefore no additional information can be deducted from these horizontal lines.

The spectrogram and standard deviation for FUT1-A8 are plotted in Fig. 3. The first extra frequency component besides the DC component appear at 390 Hz similar to FUT1-A2, but this peak appears at 169 W of output power compared to 180 W in Fig. 2. The TMIs sets in at 11 W lower output power due to the expected decrease in TMI threshold with number of test run. The TMI frequency peak at 390 Hz disappears at 172 W and then reappears at 180 W together with several additional higher harmonics. The missing frequency peak from 172 W –

#191938 - $15.00 USD Received 7 Jun 2013; revised 27 Aug 2013; accepted 4 Sep 2013; published 10 Sep 2013

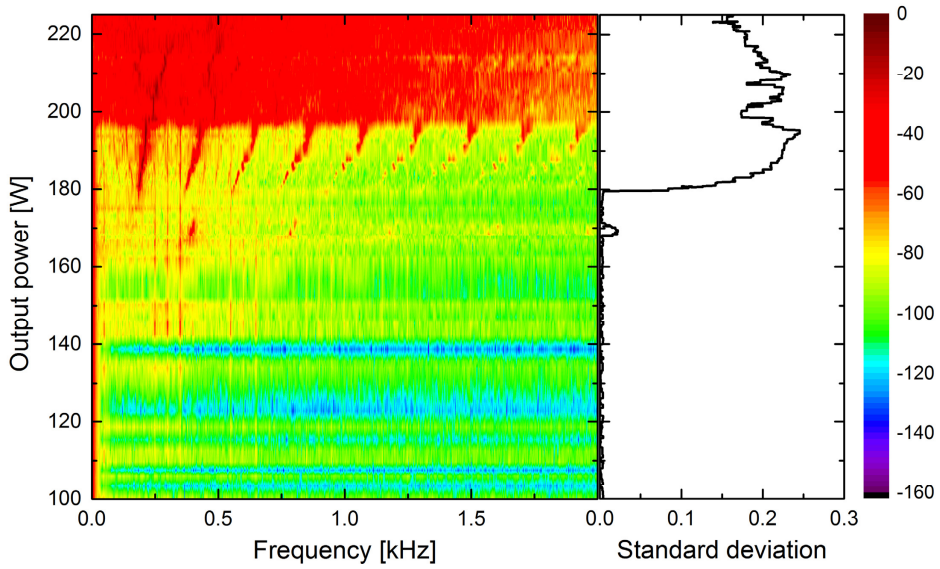

Fig. 3. Data for FUT1-A8. Fourier transformed normalized spectrogram plotted in dB for the extracted output power as a function of frequency. The standard deviation is plotted on equal power scale to the right.

180 W could be related to pinhole size, if the mode fluctuations are not occurring within the selected part of the mode profile, though the DC component is stable. The spectrogram changes character above 196 W, where it initially consisted of discrete frequency peaks it becomes a continuous span of frequencies from 196 W and up, denoted the chaotic regime. The output spectrum broadens from initially being the signal frequency in a stable regime at low power levels, to consist of discrete frequency peaks in the transition regime with TMIs, and then entering the chaotic regime with a white span of frequencies. The original discrete frequencies are weakly seen in the chaotic regime in some areas. Again a clear growth in the standard deviation in Fig. 3 is observed as soon as TMIs is detected. Notice that also the standard deviation is roughly zero from 172 W – 180 W, where the TMI frequency components disappear, and then increase abruptly at 180 W, when the components reappear.

All three recorded spectrograms from TMI repeat 1, i.e. FUT1-A2, FUT1-A8, FUT1-A15, are plotted in Fig. 4 on equal output power axis to allow for comparison. The output power level at which the first TMI frequency component appear is seen to drop with test number.

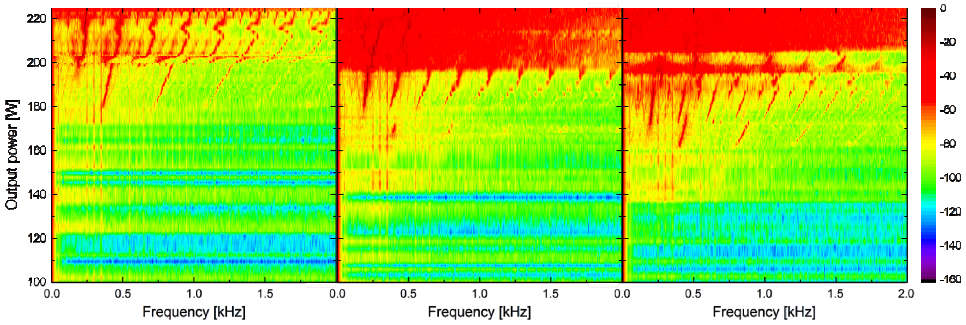

Fig. 4. Spectrogram for FUT1-A2, FUT1-A8, and FUT1-A15 plotted together for comparison.

#191938 - $15.00 USD Received 7 Jun 2013; revised 27 Aug 2013; accepted 4 Sep 2013; published 10 Sep 2013

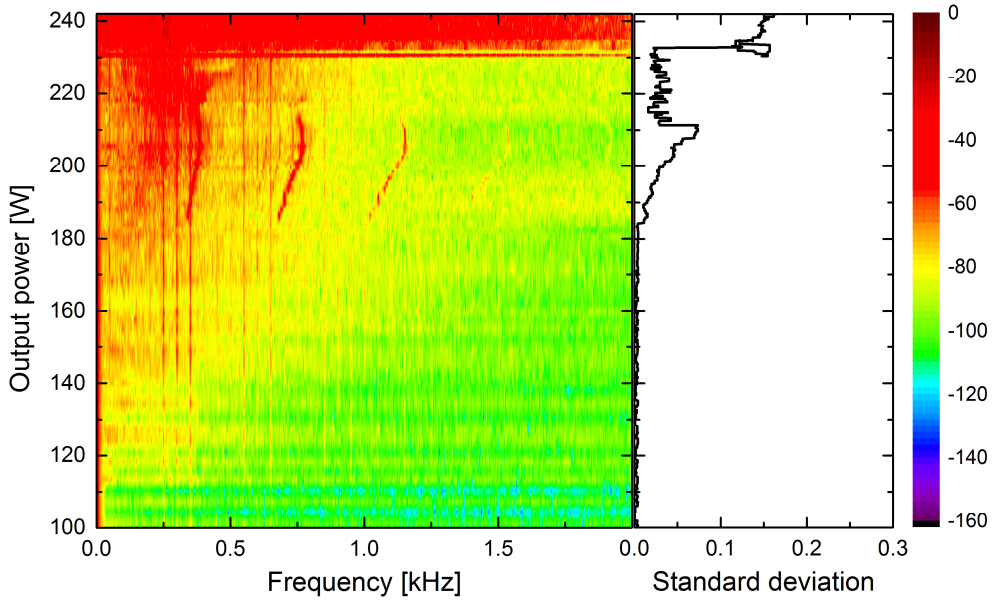

Fig. 5. Data for FUT1-C2. Fourier transformed normalized spectrogram plotted in dB for the extracted output power as a function of frequency. The standard deviation is plotted on equal power scale to the right.

FUT1 is thermally annealed after 15 tests in TMI repeat 1 to remove color centers created under the tests: TMI anneal. The output end of the 281/100 rod fiber is heated to 300⌡C for 2 h and slowly cooled down. A new set of tests is performed: TMI repeat 2.

The spectrogram and standard deviation for FUT1-C2 is plotted in Fig. 5 similar to Fig. 2 and Fig. 3, that is test number 2 in TMI repeat 2. The first TMI generated frequency peak appears at 340 Hz at 187 W of signal power, which is 7 W higher than FUT1-A2 in Fig. 2. Again the second, third and fourth harmonics are visible at 680 Hz, 1020 Hz, and 1370 Hz in Fig. 5, and a similar drift in frequency with increased pump power is observed. The TMI regime changes from transient to chaotic at 231 W. The standard deviation grows when TMI components appear, however not as abruptly as observed in TMI repeat 1. The discrete frequency peaks are vague between ~220 W – 231 W, which is also reflected in the lower standard deviation recorded by the pinholed photodiode. At 231 W of output power the standard deviation instantly increases as the output enters the chaotic regime.

The three spectrograms from TMI repeat 2, i.e. FUT1-C2, FUT1-C8, FUT1-C15, are plotted together in Fig. 6 on equal output power axis for comparison. Again the TMI

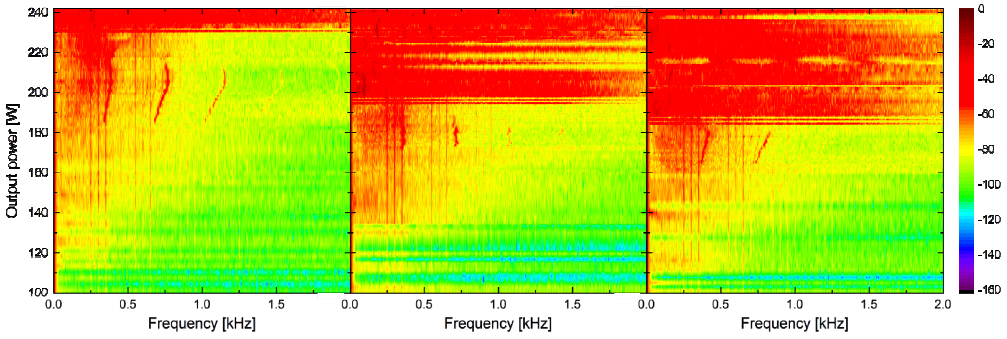

Fig. 6. Spectrogram for FUT1-C2, FUT1-C8, and FUT1-C15 plotted together for comparison.

#191938 - $15.00 USD Received 7 Jun 2013; revised 27 Aug 2013; accepted 4 Sep 2013; published 10 Sep 2013

frequency components are observed to appear at lower output power with test number. Also the transition from the transient to chaotic regime occurs at decreasing output power.

The vertical noise lines are visible in all spectrograms especially three lines at 250 Hz, 300 Hz, and 350 Hz with a frequency spacing of 50 Hz. These are attributed to a progression of the European utility frequency of 50 Hz. The first TMI frequency peaks appear at 360 Hz, 390 Hz and 340 Hz in Fig. 2, 3, and 5, all close to a vertical noise line. One theory of TMIs by Hansen et *al.* [15] predicts that TMIs can be seeded by system noise instead of quantum noise, which means that the vertical noise lines in the spectrograms could initiate coupling between the FM and HOM by sideband modulation of the signal. In TMI repeat 2 the noise lines are amplified and appear more evident compared to TMI repeat 1.

4. Transverse mode instability threshold definition

Three regimes are identified from the spectrograms for the 285/100 rod fiber as the extracted output power increases. Initially the fiber is in a stable regime with a Gaussian-like FM output centered around 0 Hz in the spectrograms. At the onset of TMI an extra frequency component appears that creates higher harmonics, resulting from fluctuations in the modal output recorded by the pinholed photodiode. At onset these fluctuation are too vague to be observed by the CCD camera, but are clearly visible in the spectrogram. The TMI components appear as discrete frequencies in the transient regime with the components shifting to higher frequencies for increased output power, as well as the first TMI component roughly appearing on the same noise line at 350 Hz in all 6 spectrograms. For higher output power the output becomes a continuous span of frequencies in the chaotic regime. The power threshold for each regime decreases as the fiber is tested multiple times, visible in Fig. 4 and Fig. 6. However thermally annealing the fiber recovers the TMI threshold to the level of the pristine fiber, yielding a stable FM output again for high extracted output power.

The measured standard deviations increase as soon as TMI frequency components appear in the spectrograms in Fig. 4 and Fig. 6, and are plotted together in Fig. 7. The increase seems to be rather abrupt and step like, and not exponential as observed by Otto et al. in [12]. This leads to a simple definition of the TMI threshold as the output power level where the standard deviation becomes larger than 0.01 indicated by the dashed line in Fig. 7.

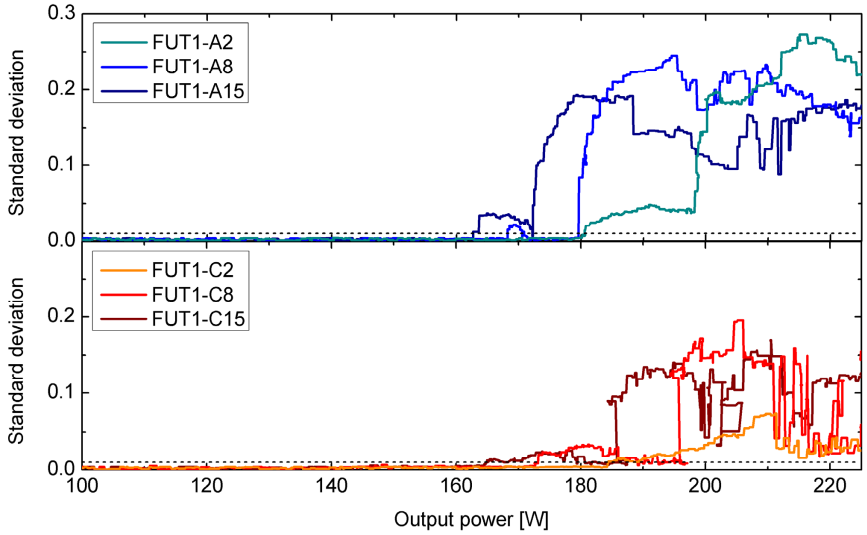

Fig. 7. Standard deviation as a function of extracted output power for TMI repeat 1 (top) and TMI repeat 2 (bottom). TMI threshold is defined at the level where the standard deviation reaches 0.01 indicated by the dashed line.

#191938 - $15.00 USD Received 7 Jun 2013; revised 27 Aug 2013; accepted 4 Sep 2013; published 10 Sep 2013

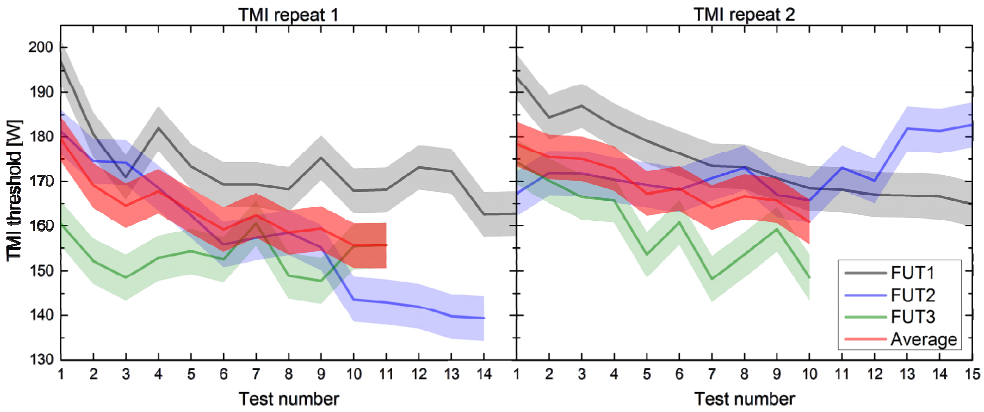

Fig. 8. Measured TMI threshold as function of test number in TMI repeat 1 and 2.

The TMI thresholds for all tests are determined based on measured standard deviation for FUT1, FUT2, and FUT3, and plotted in Fig. 8, altogether a total of 80 measurements. The power meter in the setup might cause an uncertainty on the exact output power level estimated to ± 5 W, due to response time, and indicated in Fig. 8. The TMI threshold decreases with test number in TMI repeat 1 as also observed in [3]. After which the rod fibers are thermally annealed to recover the TMI threshold to the initial power level. Again a decrease in TMI threshold is observed in TMI repeat 2 for FUT1 and FUT3 as expected. For FUT2 the TMI threshold seems to stay constant up to test 10, and then increase with test number for test 10 - 15. There are uncertainties with the measurement technique that might result in the observed TMI threshold increment. First of all the transient regime changes character during one TMI repeat, which is apparent when comparing the spectrograms in Fig. 4 and Fig. 6, causing the standard deviation to change. This could be the reason for the increase in TMI threshold with test number for FUT2. Secondly, deviations in standard deviation are related to size and position of the pinhole in front of the photodiode, as mentioned previously. A too closed pinhole could result in a higher TMI threshold, if the beam at TMI onset fluctuates between positions at the core edge resembling LP11-like mode maxima, which are not detected by the pinholed photodiode. On the other hand a too large pinhole would allow the entire core light to be detected by the photodiode despite fluctuations, making beam fluctuations not measurable, which severely affect TMI threshold determination.

The average TMI threshold of TMI repeat 1 decreases from 180 W – 156 W over the first 10 tests, A1 – A10. The TMI threshold is recovered between TMI repeat 1 and TMI repeat 2 by the thermal annealing to an average value of 178 W in the first test of TMI repeat 2, C1, and decreases with test number to 161 W in test 10 of TMI repeat 2, C10. The difference between TMI threshold of A1 and C1 is 2 W, less than the estimated uncertainty of the power meter, thus the TMI threshold seems fully recovered by thermal annealing. The average TMI threshold also decays to approximately the equal output powers, 156 W and 161 W, after 10 tests in TMI repeat 1 and 2 confirming the trend of TMI threshold decay with test number.

The TMI frequency components appear roughly on top of the noise line at 350 Hz in the 6 spectrograms in Fig. 4 and Fig. 6, indicating that the noise level might influence the TMI threshold. Noise variations could lead to TMI threshold variations showing up as uncertainties in Fig. 8. Externally generated noise could also interfere momentarily with the measurement affecting the TMI threshold.

5. Conclusion

The properties of TMIs have been investigated by testing three 285/100 rod fibers in a single-pass amplifier setup reaching up to ~200 W of extracted output power without beam instabilities. The pump power was increased during testing well above the threshold for TMI

#191938 - $15.00 USD Received 7 Jun 2013; revised 27 Aug 2013; accepted 4 Sep 2013; published 10 Sep 2013

to uncover TMI dynamics and to set a simple definition for TMI threshold. The fibers were tested in three steps: One TMI repeat consisting of minimum 10 tests performed on initially pristine fibers, followed by one thermal annealing step, TMI anneal, where the fibers were heated to 300⁰C for 2 h to thermally recover the TMI threshold. Hereafter another TMI repeat was performed to investigate the TMI dynamics and threshold again. Three different regimes for the output were identified with increasing pump power. The stable regime, having an FM Gaussian-like output with a DC component centered at 0 Hz, is on average below ~180W. A second frequency was generated apart from the DC component, when TMIs set in as harmonic beam oscillations between the FM and first HOM at TMI threshold. Higher harmonic beam fluctuations of this frequency are observed with increasing output power as long as the fiber is operated in the transient regime. Further increase in output power changed the regime to chaotic, where the beam fluctuations consisted of a white continuum of frequencies. The TMI frequency components were observed to originate on top of system noise speculated to be electrical noise lines, and we believe that the electrical amplitude noise triggers the onset of TMI. A pinholed photodiode measured standard deviation, which was seen to increase abruptly in a step-wise manner at TMI onset. This led to the simple definition of TMI threshold at the output power where the standard deviation reached 0.01. The 285/100 rod fibers had a TMI threshold that decayed with the number of performed tests, but could be fully recovered by a thermal annealing step in the experimental procedure.

#191938 - $15.00 USD Received 7 Jun 2013; revised 27 Aug 2013; accepted 4 Sep 2013; published 10 Sep 2013